Korea-Australia Rheology Journal
Vol. 15, No. 2, June 2003 pp. 97-105

Nonlinear response of complex fluids under LAOS (large amplitude oscillatory shear) flow

Kyu Hyun, Jung Gun Nam, Manfred Wilhelm[1], Kyung Hyun Ahn* and Seung Jong Lee
School of Chemical Engineering, Seoul National University San 56-1 Shillim-dong, Gwanak-gu, Seoul 151-744, Korea
[1]Max-Planck Institut für Polymerforschung, Postfach 3148, 55021 Mainz, Germany

(Received April 4, 2003; final revision received June 2, 2003)

Abstract

In the previous paper (Hyun *et al.*, 2002), we have investigated the shape of storage modulus (G') and loss modulus (G") of complex fluids under large amplitude oscillatory shear (LAOS) flow. As the strain amplitude increases, however, the stress curve becomes distorted and some important information may be smothered during data processing. Thus we need to investigate the stress data more precisely and systematically. In this work, we have obtained the stress data using high performance ADC (analog digital converting) card, and investigated the nonlinear response of complex fluids, 4wt% xanthan gum (XG), 2 wt% PVA/ 1 wt% Borax, and 1 wt% hyaluronic acid (HA) solutions, using Fourier transformation (FT) rheology. Comparing the strain signals in time domain with FT parameters in frequency domain, we could illustrate the sensitivity and importance of FT rheology. Diverse and unique stress patterns were observed depending on the material system as well as flow environment. It was found that they are not the outcome of experimental deficiency like wall slip but characteristics of the material system. When nonlinear response of complex fluids is analyzed, the intensity and phase angle of higher harmonic contributions should be considered together, and the shape of the stress signal was found to be strongly dependent upon phase angle.

Keywords **:** complex fluids, LAOS, FT rheology, ADC cards, Xanthan Gum, PVA/Borax, hyaluronic acid

1. Introduction

Recently there has been a growing interest in complex fluids, which include biological macromolecules, polyelectrolytes, surfactants, suspensions, emulsions, and so on (Larson, 1999). These fluids are used in many fields of industry such as foods, personal care products, electronic and optical materials and for many biological applications. When exposed to flow environment, complex fluids show interesting behavior such as shear thickening, flow induced association, etc. These behaviors result from the conformational change of a single or a group of polymer chains, or from the microstructural changes. The amount of salt, pH, temperature or external field may affect the behavior depending on situation.

Large amplitude oscillatory shear (LAOS) is a useful test for such a fluid because strain amplitude and frequency can be varied independently allowing a broad spectrum of conditions to be attained (Yosick *et al.*, 1997). Moreover, because oscillatory shear does not involve any sudden jump in speed or position, it is a relatively easy flow to generate (Giacomin and Dealy, 1993). From previous research (Hyun *et al.*, 2002), we observed that there exist at least 4 types of LAOS behavior of complex fluids from experiments. It is also reported that there exist 4 generic types of LAOS behavior from the network theory (Sim *et al.*, 2003; Kim *et al.*, 2002). Thereby, we have proposed LAOS test as a way to classify the complex fluids.

However, LAOS test has a disadvantage; the stress output is not purely a single sinusoidal any more and the behavior can no longer be described in terms of storage modulus and loss modulus due to higher harmonic contributions (Dealy and Wissbrun, 1990).

When strain amplitude is large, the stress becomes no longer sinusoidal and has higher harmonic contributions,

$$\sigma(t) = \sum_{n=1,odd} \sigma_n \sin(n\omega_1 t + \phi_n) \tag{1}$$

where the magnitude σ_n and the phase angle ϕ_n depend on strain amplitude and imposed frequency ω_1 (Giacomin and Dealy, 1993). Recently, in order to analyze higher harmonic contributions in LAOS, "high sensitivity Fourier transform rheology" method has been introduced (Wilhelm *et al.*, 1998; 1999; 2000; Wilhelm, 2002). Fourier transformation (FT) rheology decomposes stress data in time domain into frequency dependent spectrum. Van Dusschoten *et al.* (2001) proposed a method which increases the

*Corresponding author: ahnnet@snu.ac.kr

sensitivity of torque transducer via oversampling technique using a high performance ADC (analog digital converter) card. The basic idea is to acquire the oscillatory shear data at the highest possible acquisition rate as allowed by a modern ADC card. The sampling rate may exceed 50kHz with this method even for a low frequency shear experiment. In a second step, the raw time data is truncated "on the fly" by means of a so-called "boxcar" average method over, e.g., several hundreds or thousands of raw data points (Skoog and Leary, 1992).

In the previous paper, we focussed on the shape of storage modulus (G') and loss modulus (G") of complex fluids. Now we will investigate the stress data more precisely because some important information can be smothered during the data processing. Therefore, the purpose of this work is to obtain the nonlinear stress data using high performance ADC card, and investigate the nonlinear response of complex fluids using Fourier transformation rheology. We also investigate the shape of the stress signal as a function of time, in relation to polymer structure. Since wall slip may exist when large strain amplitude is imposed, we also compare the stress data from both normal and sand papered fixtures to verify the effect of wall slip.

2. Experiments

2.1. Materials and sample preparation

Poly(vinyl alcohol)/Borax

Poly(vinyl alcohol) (PVA) is a unique synthetic polymer having a large number of hydroxyl groups that can react with other functional groups. PVA sample used in this study was purchased from Sigma-Aldrich Co. The average molecular weight is 124,000-186,000, and the degree of hydrolysis is 98-99%. Borax is sodium borate ($Na_2B_4O_7$ $10H_2O$), a small amount of which produces a remarkable increase in viscosity when it is added to PVA aqueous solution. This is due to the formation of a complex between hydroxyl groups and borate anions, which plays a role as a temporary crosslinking among PVA chains (Inoue and Osaki, 1993; Hyun *et al.*, 2002). 2 wt% PVA and 1 wt% Borax were dissolved in dust-free purified water, and then the solution was homogenized by rotating at 300 rpm for about 2 hours at 80°C.

Hyaluronic acid

Hyaluronic acid (HA) or hyaluronan is natural biocompatible and biodegradable linear polysaccharide composed of repeating disaccharide units of D-glucoronic acid and N-acetyl-D-glucosamine linked at 1,3 and 1,4 position, respectively. HA is present in all soft tissues of higher organism, and in particular in the synovial fluids and vitreous humor of eyes (Laurent and Fraser, 1992). HA sample used in this study was donated by LGLS Ltd. Molecular weight is about 3,300,000. The sample was dissolved in water, and then the solution was homogenized by rotating at 300 rpm for about 3 hours at 40°C. The concentration of HA solution was 1 wt%.

Xanthan Gum

Xanthan gum (XG) is a high molecular weight expolysaccharide produced by bacterium Xanthomonas Compestirs. XG sample used in this study was purchased from Sigma-Aldrich Co. XG was dissolved in dust-free purified water for 1 day at room temperature, and then the solution was homogenized by rotating at 300rpm for about 2 hours at 60°C. XG concentration was 4 wt%.

2.2. Experimental methods

Rheological measurements were carried out on a strain-controlled rheometer (RMS 800, Rheometrics Inc.) using parallel plate and cone-and-plate (cone angle 0.04 radians, gap 50 μm) fixtures with a diameter of 50 mm and lower plate with a dam. Silicone oil (kinematic viscosity is 10cs at 25°C) was used to prevent water evaporation. Strain sweep test was carried out in the strain range from 1% to 1000% at a fixed frequency of 1rad/s at 25°C. For the raw data acquisition, a 16bit ADC card (PCI-6052E; National Instruments, Austin, USA) with a sampling rate up to 333kHz was used. This ADC card was plugged into a stand-alone PC equipped with LabView software (National Instruments).

3. Results and discussion

3.1. Fourier transformation

As the strain amplitude is increased in the oscillatory shear flow, the stress signal becomes no longer sinusoidal. This means that the stress signal has higher harmonic contributions. These contributions were analyzed by Fourier transformation. Fourier transformation decomposes a waveform or function in time domain into frequency dependent spectrum, then it sums to the original waveform with the stress response. An example of Fourier transformation is shown in Fig. 1. Fig. 1(a) shows the raw data of XG 4% solution at $\omega_1 = 1$ Hz and strain amplitude γ_0=25%. Fig. 1(b) shows higher harmonic contributions, which have been obtained by Fourier transformation. From these figures, it is confirmed that the stress signal has higher harmonic contributions. For non-Newtonian materials, the application of oscillatory shear with a single frequency results in the generation of odd higher harmonic contributions (Giacomine and Dealy, 1993; Wilhelm *et al.*, 1998). However, we observe additionally a small peak at 2 ω_1. The existence of even harmonics has rarely been reported. The occurrence of even frequency components in the response signal often results from experimental insufficiencies (Onogi *et al.*, 1970). Wall slip is supposed to be the main reason for the occurrence of even harmonic (Reimers and Dealy, 1996). Wilhelm *et al.* (1998) explained the appearance of even harmonics arising from

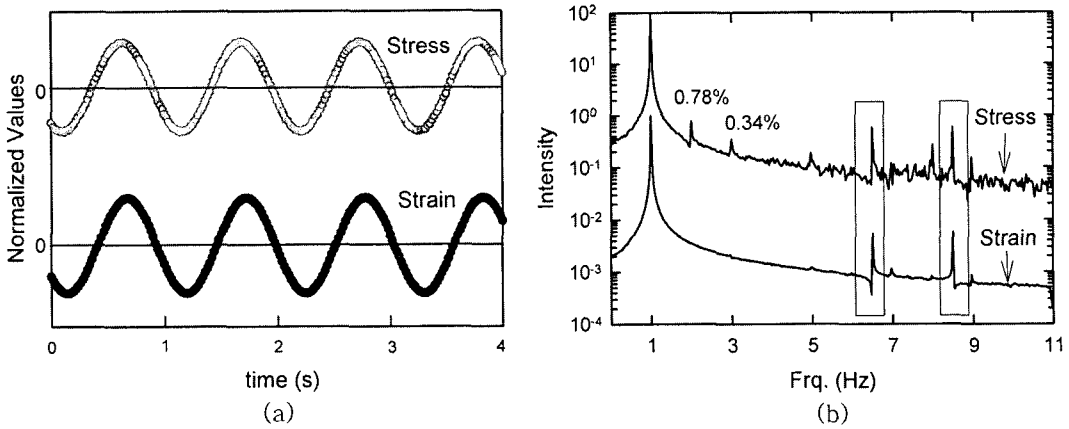

Fig. 1. (a) Raw data and (b) Fourier spectra of stress and strain curves obtained with 4 wt% XG solution under oscillatory deformation at ω=1 *Hz* and strain amplitude γ_0=25%.

time-dependent memory effect or non-linear elastic contribution in the system. Recently, Sagis *et al.* (2001) have explained the appearance of even harmonics by incorporating an orientation tensor which represents anisotropic internal microstructure. Their experimental data of xanthan gels also showed even harmonics. However, the origin is not yet completely understood, and the phenomenon is of further interest.

In case of strain, which is controlled by the rheometer, the Fourier spectrum should not show higher harmonic contributions. The strain curve indeed shows sinusoidal shape as in Fig. 1(a), however there appear peaks at higher frequencies as indicated in rectangular box in Fig. 1(b) at around 6 and 8Hz. This is most probably caused by a defect of the motor. It means that the Fourier transformation rheology is very sensitive enough to reveal a small defect of the motor. The defect affects the stress signal though it is not detectable in the stress curve, but FT rheology is sensitive enough to detect a small distortion of the stress signal. This may be a good illustration of the inherent sensitivity of FT rheology.

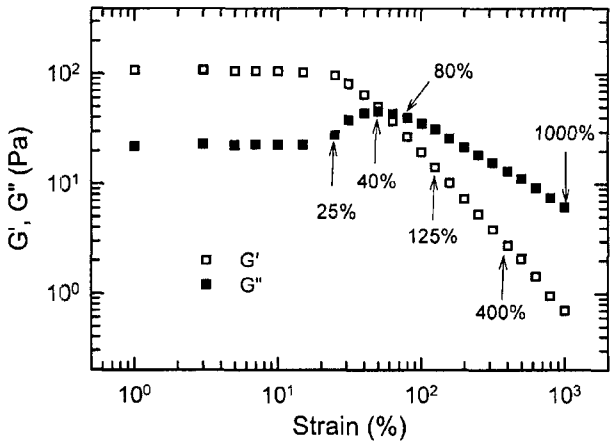

Fig. 2. Storage modulus (G') and loss modulus (G") of XG solution as a function of strain amplitude at a fixed frequency (1 rad/s). Open symbol (○) is storage modulus (G') and filled symbol (●) is loss modulus (G"). G' decreases and G" shows an overshoot (type III: weak strain overshoot). The stress data at selected strain amplitudes are shown in Fig. 3.

3.2. Xanthan Gum

Fig. 2 shows storage modulus (G') and loss modulus (G") of xanthan gum solution as a function of strain amplitude. Storage modulus (G') decreases, and the loss modulus (G") increases followed by decreasing as strain amplitude increases. Hyun *et al.* (2002) defined this behavior as type III (weak strain overshoot). We selected 6 strain amplitudes (γ_0 = 25%, 40%, 80%, 125%, 400%, 1000%) in Fig. 2, and then plotted the corresponding stress signals in Fig. 3. From the figure, it is confirmed that the stress signal is distorted more and more as strain amplitude increases. At strain amplitude γ_0 = 25%, the stress signal is nearly sinusoidal and the Lissajous pattern (stress vs. strain) is elliptical. At a larger amplitude γ_0 = 40%, the stress signal is a little tilted forward with a sinusoidal shape, and the Lissajous pattern is distorted from ellipsoid to a rounded parallelogram. When the strain amplitude is increased to γ_0 = 80%, the stress signal becomes "saw-tooth" shape and a small peak appears at the position of maximum and minimum stress. The Lissajous pattern becomes lozenge-shape. As strain amplitude increases further, the stress becomes more distorted and the small peak becomes pronounced more and more. This unique behavior may be related to the structure of xanthan gum polymer chains. The structure of xanthan is based on a linear 1,4β-D-glucose backbone with charged trisaccharide side chains on every second residue. In aqueous solution at 25°C, the backbone of xanthan is disordered but highly extended due to electrostatic repulsion from the charged groups on the side chains. Due to the highly extended structure, the mol-

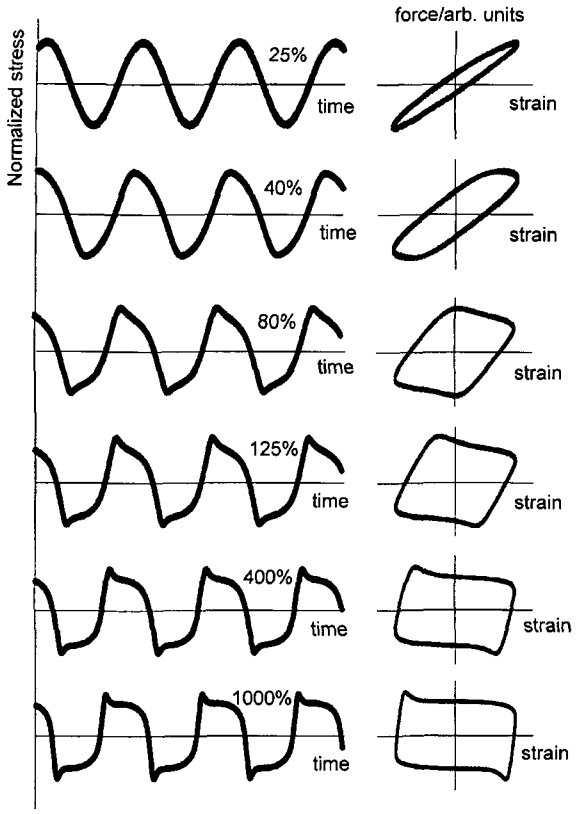

Fig. 3. The stress data of XG solution obtained at a fixed frequency (1 rad/s) but different strain amplitudes are plotted on the left hand side, and the corresponding Lissajous patterns (stress vs. strain) are shown on the right hand side.

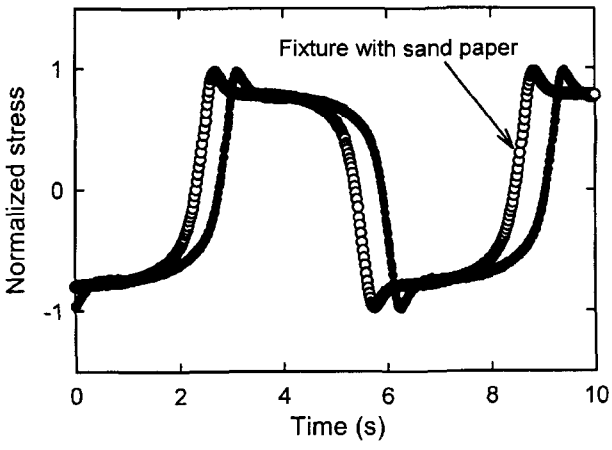

Fig. 4. The stress data of XG solution with normal (filled circle) and sand paper attached (open circle) parallel plate fixtures are compared. The stress data have been shifted arbitrarily for comparison.

ecules may align and associate (partly due to hydrogen bonding) to form a weakly structured material (Rochefort and Middleman, 1987).

Graham (1995) stated that the small peak in the stress signal at high strain amplitude is caused by wall slip, and

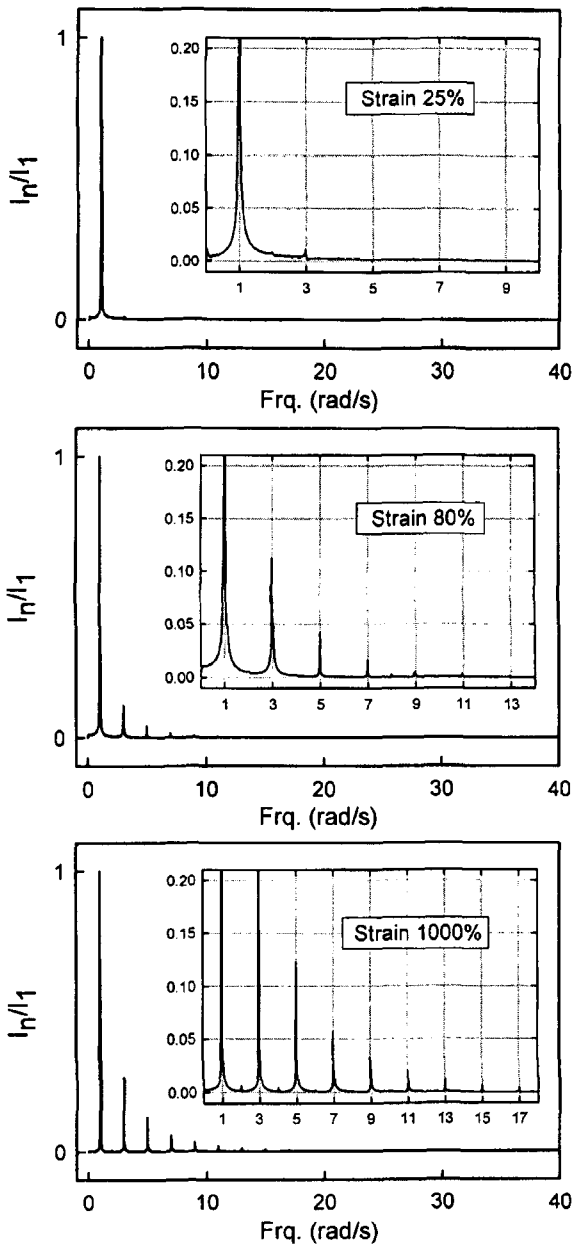

Fig. 5. Fourier spectra of the stress response obtained with XG solution subjected to oscillatory deformation at 1 rad/s. Applied strain amplitudes are γ_0=25, 80, and 1000%, respectively. The intensity has been normalized by the intensity of the fundamental frequency.

that the possibility of wall slip becomes larger as the strain amplitude increases. To verify the effect of wall slip, we carried out experiments, using parallel plates with a sand paper attached on the plate surfaces. We compared the stress signals from normal and sand papered fixtures at strain amplitude 1000% in Fig. 4. The stress signal has been shifted arbitrarily for comparison. The two signals overlap, and the curves of G' and G" coincide too. Thus, we think that the stress peak is not due to wall slip, but it

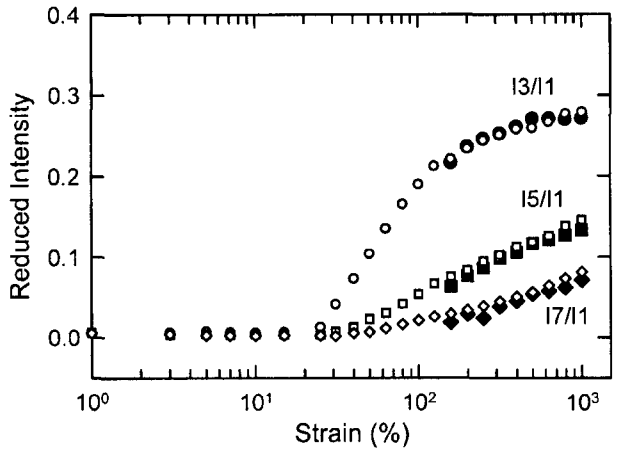

Fig. 6. The higher harmonics of XG solution as a function of strain amplitude. Open circle is obtained from normal parallel plate fixture, and filled circle is obtained from sand paper attached parallel plate fixture.

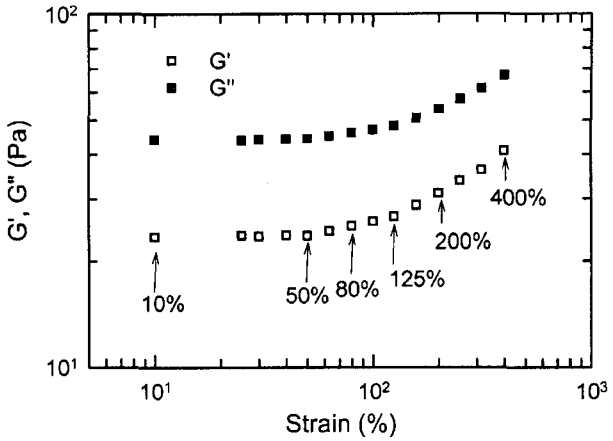

Fig. 7. Storage modulus (G') and loss modulus (G") of PVA/Borax solution as a function of strain amplitude at fixed frequency (1 rad/s). Open symbol (○) is storage modulus (G') and filled symbol (●) is loss modulus (G"). G' and G" increases after critical strain amplitude (type II: strain hardening).

is a characteristic peak of XG solution

In order to quantify the extent of non-linear response when subjected to oscillatory shear at a fixed frequency, Fourier analysis of the stress response has been carried out. The Fourier spectra are shown in Fig. 5. It is clear that the intensity of higher harmonics increases as strain amplitude increases. Fig. 6 shows the normalized intensity as a function of strain amplitude. In Fig. 6, filled symbols are the results of sand papered fixture and open symbols are the results from normal plates. The results almost coincide, and it is again confirmed that the distortion of stress signal does not result from wall slip. The point of strain amplitude $\gamma_0 = 23\%$, where the higher harmonics start to increase significantly, is in good agreement with the onset of non-linear regime obtained from the curve of G' and G" versus strain amplitude. However, it has been reported that the presence of high harmonics is a more sensitive indicator of nonlinearity than the curves of G' and G" versus strain (Reimmers and Dealy, 1996).

3.3. PVA/Borax

Fig. 7 shows G' and G" of PVA/Borax solution as a function of strain. Storage modulus (G') and loss modulus (G") increase as strain amplitude increases. Hyun *et al.* (2002) defined this behavior as type II (strain hardening). In Fig. 7, we selected 6 strain amplitudes ($\gamma_0 = 10\%$, 50%, 80%, 125%, 200%, 400%) and plotted the corresponding stress signals in Fig. 8. From the figure, the distortion of stress signal is rarely observed and the Lissajous pattern shows the same pattern as strain amplitude increases. In Fig. 9, reduced intensity as a function of strain amplitude is shown. The intensity of the third harmonic increases as strain amplitude increases but it is less than 5%.

The PVA/Borax solution shows strain hardening (G' and G" increasing) behavior. The origin of strain hardening is

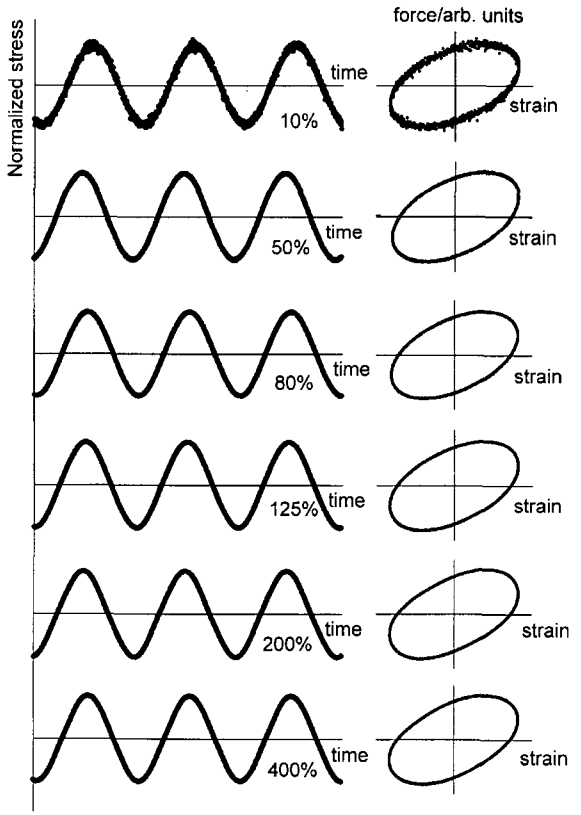

Fig. 8. The stress data of PVA/Borax solution obtained at a fixed frequency (1 rad/s) but different strain amplitudes are plotted on the left hand side, and the corresponding Lissajous patterns (stress vs. strain) are shown on the right hand side.

the network formation. The network structure is strong and permanent chemical bonding between PVA chain and

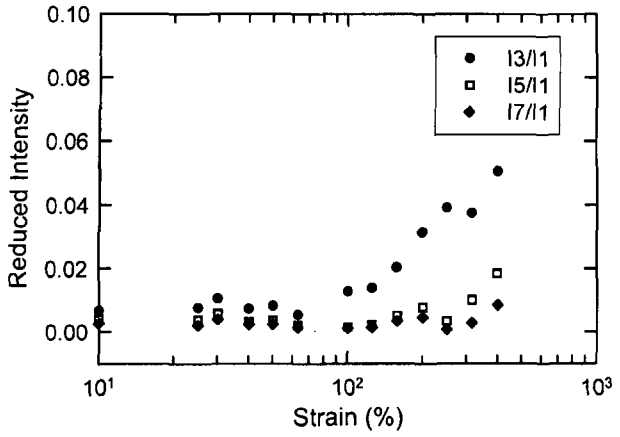

Fig. 9. The higher harmonics of PVA/Borax solution as a function of strain amplitude.

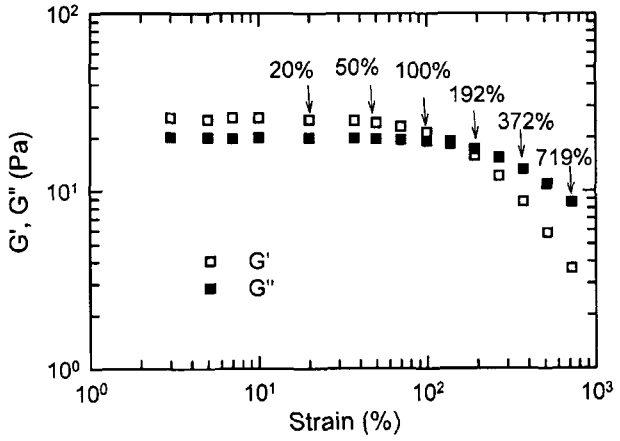

Fig. 10. Storage modulus (G') and loss modulus (G") of HA solution as a function of strain amplitude at fixed frequency (1 rad/s). Open symbol (○) is storage modulus (G') and filled symbol (●) is loss modulus (G"). G' and G" decrease after critical strain amplitude (type I: strain thinning).

Borax (Hyun *et al.*, 2002; Inoue and Osaki, 1993). The strong network resists against flow, and G' and G" increase as strain amplitude increases. However, there seems to be no strain-induced microstructural change, because the severe distortion of stress signal is not observed in this case.

3.4. Hyaluronic acid (HA)

Fig. 10 shows G' and G" of HA solution as a function of strain. Storage modulus (G') and loss modulus (G") decrease at high strain amplitudes. Hyun *et al.* (2002) defined this behavior as type I (strain thinning). The stress signals and Lissajous figures at different strain amplitude are plotted in Fig. 11, and the reduced intensity as a function of strain amplitude is given in Fig. 12. At strain amplitude $\gamma_0 = 100\%$ the distortion of stress signal is not observed, however the third harmonic starts to increase at strain amplitude $\gamma_0 = 100\%$ as shown in Fig. 12. This again

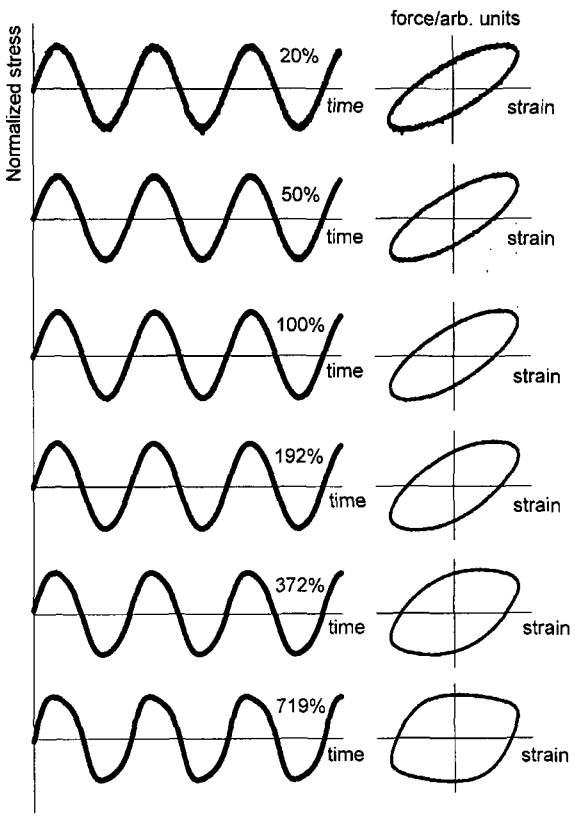

Fig. 11. The stress data of HA solution obtained at a fixed frequency (1 rad/s) but different strain amplitudes are plotted on the left hand side, and the corresponding Lissajous patterns (stress vs. strain) are shown on the right hand side.

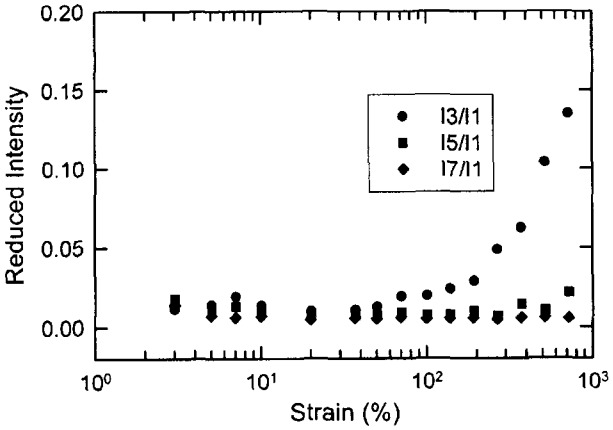

Fig. 12. The higher harmonics of HA solution as a function of strain amplitude.

asserts that the FT parameter is a sensitive indicator of the onset of nonlinearity. The stress signal of HA solution at 719% is similar to that of XG solution at strain amplitude 80%. The shape is forward tilted "saw-tooth" type, and the difference is that the shape is sharper in XG than in HA. Both XG and HA are a kind of polysaccharide, so the main

chain of each polymer is very similar. However, XG has functional side chains but HA does not (Hyun *et al.*, 2002). Due to side chains, which form weakly structured material, XG solution shows a small sharp peak at the position of maximum and minimum stresses, while HA solution shows less sharp "saw-tooth" stress signal. It is apparent that the shape of stress signal is closely related to the structure of the polymer chains in solution.

3.5. Phase angle

The stress can be expressed in terms of intensity and phase angle as shown in Eq. (1). With the idea of Neidhofer *et al.* (2002), the stress signal can be reformulated as follows after substituting time t by $t = t' - \phi_1/\omega_1$,

$$\sigma(t') \propto a_1 \sin(\omega_1 t') + a_3 \sin(3\omega_1 t' + \phi'_3) + a_5 \sin(5\omega_1 t' + \phi'_5) + \cdots \quad (2)$$

where $\phi'_n = \phi_n - n\phi_1$ is the relative phase angle.

Let us assume that the intensity of the third harmonic is 10% of the first harmonic and the harmonics higher than three are negligible, then Eq. (2) becomes

$$\sigma(t') \propto \sin(\omega_1 t') + 0.1^* \sin(3\omega_1 t' + \phi'_3) \quad (3)$$

Now we change the relative phase angle ϕ'_3 and investigate the shape of the stress signal. Then we can obtain some information on the phase angle, and the results are plotted in Fig. 13. Although the intensity of the 3rd harmonic is the same, the stress signal shows remarkably different shape as the relative phase angle changes. In case of $\phi'_3 = 0$, the stress signal shows plateau, and this type is observed in diblock copolymer gel (Daniel *et al.*, 2001) as well as in our own experiments with PEO-PPO-PEO triblock copolymer hard gel. The "forward tilted shoulder" is observed in XG and HA solutions as observed in Fig. 3 and Fig. 11. The "backward tilted shoulder" can be found in our own experiments with PEO-PPO-PEO soft gel. The

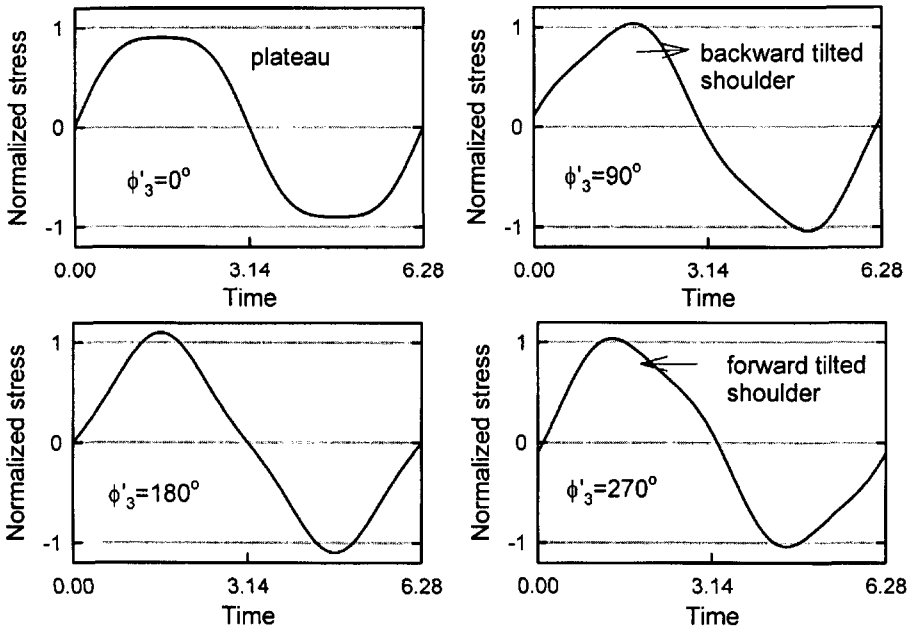

Fig. 13. The normalized stress data ($\sigma(t') \propto \sin(\omega_1 t') + 0.1^* \sin(3\omega_1 t' + \phi'_3)$) at different third relative phase angle ϕ'_3.

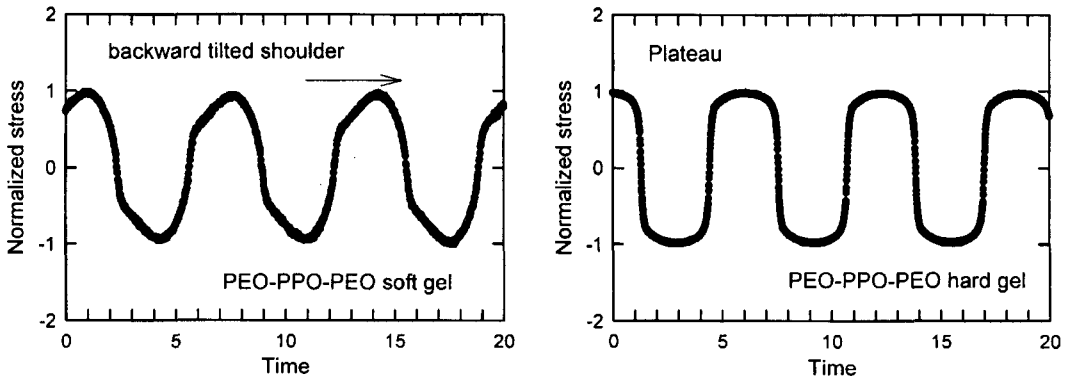

Fig. 14. The stress data of PEO-PPO-PEO soft gel and hard gel as a function of time.

stress signals of above-mentioned PEO-PPO-PEO hard gel and soft gel are shown in Fig. 14. In order to explain the distortion of the stress signal, we need to have both intensity and phase angle. From this approach, it seems that phase angle is more closely related to the shape of stress curve. Neidhofer *et al.* (2002) investigated higher harmonics and relative phase angle with linear PS solution and four-arm star PS melt. They found that relative phase angle is a sensitive parameter about the polymer structure. The solutions that have different microstructures like XG, PEO-PPO-PEO triblock copolymer gels, have their own unique stress shapes, and the shape of the stress signal is strongly dependent upon phase angle.

4. Conclusions

In this work, we obtained the stress signal of complex fluids under LAOS using the oversampling technique with a high performance ADC card, and the stress data were analyzed using Fourier transformation rheology. We investigated three complex fluids; 4 wt% xanthan gum (XG), 2 wt% PVA/1 wt% Borax (PVA/Borax), and 1 wt% hyaluronic acid (HA) solutions. Comparing the strain signals in time domain with FT parameters in frequency domain, we could illustrate the sensitivity and importance of FT rheology. Diverse and unique stress patterns were observed depending on the material system as well as flow environment. In case of XG solution, we found unique stress patterns as strain amplitude increases. In order to ensure whether the unique stress pattern is due to wall slip or not, we also obtained the stress data using sand paper attached parallel plate. The stress data were not different from the data with normal parallel plate. So, the unique stress pattern of XG solution is not attributed to wall slip but a characteristic stress pattern caused by the microstructure of xanthan.

PVA/Borax solution shows almost similar sinusoidal stress curve as the strain amplitude increases. The Fourier transformation analysis shows that the intensity of the third harmonic is less than 5% of the first harmonic. The PVA/Borax solution forms a network structure, which is strong and permanent chemical bonding between PVA chain and Borax. The strong network resists against flow, and G' and G" increase at high strain amplitudes. As we do not observe a severe distortion of stress signal, there seems to be no strain-induced microstructural change at strain amplitude we have investigated.

HA and XG are a kind of polysaccharide. As the main chain of each polymer is very similar, they also show similar stress shape, forward tilted "saw-tooth" shape. However the stress curve of XG shows the small peak at the position of maximum and minimum stresses, but HA does not. This difference is caused by different structures. XG has functional side chains but HA does not.

The shape of the stress signal is closely related with the microstructure of polymer solutions. There are various shapes of the stress curve for different polymer solutions, e.g. plateau, forward tilted shoulder, backward tilted shoulder, and so on. Thus when nonlinear response of complex fluids is analyzed, the intensity and phase angle of higher harmonic contributions should be considered together. The shape of the stress signal was found to be strongly dependent upon phase angle.

Acknowledgement

The authors acknowledge the support from the Korea Science and Engineering Foundation through the Applied Rheology Center at Korea University in Korea. Furthermore, Professor H.W. Spiess is acknowledged for his continuous support.

References

Daniel, C., I. W. Hamley, M. Wilhelm and W. Mingvanish, 2001, Non-linear rheology of a face-centered cubic phase in a diblock copolymer gel, *Rheol. Acta* **40**, 39-48.

Dealy, J. M. and K. F. Wissbrun, 1990, Melt rheology and its rolein plastics processing: Theory and applications, VNR, NewYork, Chapter 5.

Giacomine, A.J. and J.M. Dealy, 1993, Large-amplitude oscillatory shear, in: Collyer, A.A. (Ed.), Techniques in Rheological Measurement, Chapman & Hall, London, Chapter 4.

Graham, M. D., 1995, Wall slip and the nonlinear dynamics of large amplitude oscillatory shear flows, *J. Rheol.* **39**, 697-712.

Hyun, K., S. H. Kim, K. H. Ahn and S. J. Lee, 2002, Large amplitude oscillatory shear as a way to classify the complex, *J. Non-Newtonian Fluid Mech* **107**, 51-65.

Inoue, T. and K. Osaki, 1993, Rheological properties of poly (vinyl alcohol)/sodium borate aqueous solutions, *Rheol. Acta* **32**, 550-555.

Kim, S. H., H. G. Sim, K. H. Ahn, and S. J. Lee, 2002, *Korea-Australia Rheology J.* **14**, 49-55.

Larson, R. G., 1999, The structure and rheology of complex fluids, Oxford University Press, New York.

Laurent, T. C. and J. R. E. Fraser, 1992, Hyaluronan, *FASEB J.* **6**, 2397-2404.

Neidhofer, T., M. Wilhelm, B. Debbaut and N. Hadjichristidis, 2002, FT-rheology and finite-element simulations on polystyrene solutions and melts of various topologies, *Proceedings of the 6th European Conference on Rheology*, 463-464.

Onogi, S., T. Masuda, and T. Matsumoto, 1970, Nonlinear behavior of viscoelastic materials. I: Disperse systems of polystyrene solution and carbon black, *Trans. Soc. Rheol.* **14**, 275-294.

Reimers, M. J. and J. M. Dealy, 1996, Sliding plate rheometer studies of concentrated polystyrene solutions: Large amplitude oscillatory shear of a very high molecular weight polymer in diethyl phthalate, *J. Rheol.* **40**, 167-186.

Rochefort, W.E. and S. Middleman, 1987, Rheology of xanthan gum: salt, temperature, and strain effects in oscillatory and

steady shear experiments, *J. Rheol.* **31,** 337-369.

Sim, H. G., K. H. Ahn and S. J. Lee, 2003, Large amplitude oscillatory shear behavior of complex fluids investigated by a network model: A guideline for classfication, *J. Non-Newtonian Fluid Mech*, accepted.

Skoog, D. A. and J. J. Leary, 1992, Principles of instrumental analysis, Sauders College Publishing, Fort Worth.

Van Dusschoten, D. and M. Wilhelm, 2001, Increased torque transducer sensitivity via oversampling, *Rheol. Acta* **40**, 395-399.

Wilhelm, M., D. Maring and H.W. Spiess, 1998, Fourier-transform rheology, *Rheol. Acta* **37**, 399-405.

Wilhelm, M., P. Reinheimer and M. Ortseifer, 1999, High sensitivity Fourier-transform rheology, *Rheol. Acta* **38**, 349-356.

Wilhelm, M., P. Reinheimer, M. Ortseifer, T. Neidhöfer and H.W. Spiess, 2000, The crossover between linear and non-linear mechanical behaviour in polymer solutions as detected by Fourier-transform rheology, *Rheol. Acta* **39**, 241-246.

Wilhelm, M., 2002, Fourier-transform rheology, *Macromol. Mater. Eng.* **287**, 83-105.

Yosick, J. A., A. J. Giacomin and P. Moldenaers, 1997, A kinetic network model for nonlinear flow behavior of molten plastics in both shear and extension, *J. Non-Newtonian Fluid Mech.* **70**, 103-123.